

ZIP14 and DMT1 in the liver, pancreas, and heart are differentially regulated by iron deficiency and overload: implications for tissue iron uptake in iron-related disorders

Hyeyoung Nam,¹ Chia-Yu Wang,¹ Lin Zhang,¹ Wei Zhang,¹ Shintaro Hojyo,² Toshiyuki Fukada,^{2,3} and Mitchell D. Knutson¹

¹Food Science & Human Nutrition Department, University of Florida, Gainesville, FL, USA; ²Laboratory for Homeostatic Network, RIKEN Center for Integrative Medical Sciences, Yokohama, Kanagawa, Japan; and ³Department of Allergy and Immunology, Osaka University Graduate School of Medicine, Osaka University, Yamada-oka Suita, Osaka, Japan

ABSTRACT

The liver, pancreas, and heart are particularly susceptible to iron-related disorders. These tissues take up plasma iron from transferrin or non-transferrin-bound iron, which appears during iron overload. Here, we assessed the effect of iron status on the levels of the transmembrane transporters, ZRT/IRT-like protein 14 and divalent metal-ion transporter-1, which have both been implicated in transferrin- and non-transferrin-bound iron uptake. Weanling male rats (n=6/group) were fed an iron-deficient, iron-adequate, or iron-overloaded diet for 3 weeks. ZRT/IRT-like protein 14, divalent metal-ion transporter-1 protein and mRNA levels in liver, pancreas, and heart were determined by using immunoblotting and quantitative reverse transcriptase polymerase chain reaction analysis. Confocal immunofluorescence microscopy was used to localize ZRT/IRT-like protein 14 in the liver and pancreas. ZRT/IRT-like protein 14 and divalent metal-ion transporter-1 protein levels were also determined in hypotransferrinemic mice with genetic iron overload. Hepatic ZRT/IRT-like protein 14 levels were found to be 100% higher in iron-loaded rats than in iron-adequate controls. By contrast, hepatic divalent metal-ion transporter-1 protein levels were 70% lower in iron-overloaded animals and nearly 3-fold higher in iron-deficient ones. In the pancreas, ZRT/IRT-like protein 14 levels were 50% higher in iron-overloaded rats, and in the heart, divalent metal-ion transporter-1 protein levels were 4-fold higher in iron-deficient animals. At the mRNA level, ZRT/IRT-like protein 14 expression did not vary with iron status, whereas divalent metal-ion transporter-1 expression was found to be elevated in iron-deficient livers. Immunofluorescence staining localized ZRT/IRT-like protein 14 to the basolateral membrane of hepatocytes and to acinar cells of the pancreas. Hepatic ZRT/IRT-like protein 14, but not divalent metal-ion transporter-1, protein levels were elevated in iron-loaded hypotransferrinemic mice. In conclusion, ZRT/IRT-like protein 14 protein levels are up-regulated in iron-loaded rat liver and pancreas and in hypotransferrinemic mouse liver. Divalent metal-ion transporter-1 protein levels are down-regulated in iron-loaded rat liver, and up-regulated in iron-deficient liver and heart. Our results provide insight into the potential contributions of these transporters to tissue iron uptake during iron deficiency and overload.

Introduction

Nearly all mammalian cells normally acquire iron from the plasma iron-transport protein transferrin. Cells take up transferrin in proportion to the number of transferrin receptors located at the cell surface. After transferrin binds to transferrin receptor, the complex is internalized into endosomes, which become acidified, causing iron to dissociate from transferrin. The liberated ferric iron is then reduced to ferrous iron and transported across the endosomal membrane and into the cytosol. In developing erythroid cells of the bone marrow, which acquire iron exclusively from transferrin, the transport of iron out of the endosome is mediated by divalent metal-ion transporter-1 (DMT1). This conclusion is based on the observation that mice engineered to lack DMT1 in erythroid precursor cells fail to produce normal amounts of hemoglobin.¹ Interestingly, when DMT1 was deleted globally in the mouse, the liver of neonates displayed elevated

amounts of iron and most other cell types developed normally, indicating that alternate pathways of cellular iron uptake must exist.¹ One such pathway may involve ZIP14, a member of the ZIP family of metal-ion transporters.² ZIP14 was originally described as a zinc-import protein,³ but subsequent studies found that it could also transport iron into cells.⁴ In those studies, the iron was presented as ferric citrate, a physiological form of non-transferrin-bound iron (NTBI).⁵ NTBI can appear in the plasma when the carrying capacity of transferrin becomes exceeded, such as in the iron overload disorders hereditary hemochromatosis and β -thalassemia.⁶ NTBI is rapidly cleared by the liver,⁷ and to a lesser extent by the pancreas, followed by the heart.^{7,8} The transport properties of ZIP14, along with the observation that ZIP14 is most abundant in liver, pancreas, and heart,³ have led to the hypothesis that ZIP14 transports NTBI into these organs.⁴ More recently, we found that ZIP14 is expressed in early endosomes, where it promotes the assimilation of iron from transferrin.⁹

©2013 Ferrata Storti Foundation. This is an open-access paper. doi:10.3324/haematol.2012.072314

The online version of this article has a Supplementary Appendix.

Manuscript received on June 18, 2012. Manuscript accepted on December 10, 2012.

Correspondence: mknutson@ufl.edu

Collectively, these data suggest that ZIP14 may not only function during iron overload to take up NTBI, but also under normal or iron-deficient conditions when cells take up iron via endocytosis of transferrin.

The aim of the present study was to determine how iron deficiency and overload affect the expression of ZIP14 and DMT1 in the liver, pancreas, and heart. The localization of ZIP14 in liver and pancreas was also determined. Knowledge of where ZIP14 is expressed in these organs and how ZIP14 and DMT1 are regulated *in vivo* by iron will help us to better assess the contribution of these transporters to tissue iron uptake.

Design and Methods

Animals, diets, and non-heme iron determination

Rats were made iron-deficient, iron-adequate, or iron-loaded as described previously.¹⁰ Briefly, weanling (21-day-old) male Sprague-Dawley rats were fed modified AIN-93G purified diets containing iron at 10 ppm (iron deficient, FeD), 50 ppm (iron adequate, FeA), or 18,916 ppm (iron overload, FeO) for 3 weeks. Male *Zip14* (*Slc39a14*) knockout and wild-type control mice maintained on the 129+Ter/SvJcl x C57BL/6 background¹¹ were analyzed at 6 weeks of age. Male and female hypotransferrinemic (hpx) mice and wild-type controls maintained on the BALB/cJ background were analyzed at 16 weeks of age. Homozygous hpx mice were given a weekly intraperitoneal injection of human apo-transferrin (0.6–1.8 mg) (EMD Chemicals). All mice consumed a commercial rodent diet containing 240 ppm iron (Teklad 7912, Harlan Laboratories). At the end of the studies, animals were anesthetized with vaporized isoflurane and sacrificed by exsanguination via the descending aorta. Tissues were harvested, immediately frozen in liquid nitrogen, and stored at -80°C until use. Animal protocols were approved by the University of Florida Institutional Animal Care and Use Committee. Tissue non-heme iron concentrations were determined colorimetrically after acid digestion of tissues.¹²

Generation of ZIP14 antibody

Rabbit anti-ZIP14 antiserum was generated against peptide ENEQTEEGKPSAIEVC corresponding to amino acids 138–153 of rat ZIP14. Antibodies specific to the ZIP14 peptide immunogen were affinity purified by using a peptide-agarose column of Sulfo-Link coupling gel (Pierce).

Sample preparation and western blot analysis

The preparation of samples and western blot analysis are described in the *Online Supplementary Design and Methods*.

Transfection, immunoprecipitation, and enzymatic deglycosylation

Effectene reagent (Qiagen) was used to transiently transfect HEK 293T cells with either empty pCMV-Sport2 (control) or pCMV-Sport6 containing rat ZIP14 cDNA. To immunoprecipitate ZIP14, anti-ZIP14 antibody (400 µg) was covalently linked to AminoLink Plus Coupling Resin (Thermo Scientific) and added to a Pierce Spin Column according to the manufacturer's protocol. Immunoprecipitations were performed using the Co-Immunoprecipitation Kit (Pierce) according to the manufacturer's instructions. To assess protein glycosylation, cell lysates were digested with PNGase F, which cleaves N-linked glycans. Samples were denatured in buffer containing 1% 2-mercaptoethanol and 0.5% SDS at 37 °C for 30 min and then digested for 2 h at 37 °C with PNGase F (50,000 unit/mL of sample volume or 50 units/µg protein) (New England Biolabs).

RNA isolation and quantitative reverse transcriptase polymerase chain reaction

RNA isolation, quantitative reverse transcriptase polymerase chain reaction (RT-PCR) analysis, and determination of mRNA copy number are described in the *Online Supplementary Design and Methods*.

Immunofluorescence staining of ZIP14 in liver and pancreas

Immunohistochemistry methods are described in the *Online Supplementary Design and Methods*.

Iron loading of HepG2 cells

HepG2 human hepatoma cells were maintained as described previously.⁹ To load the cells with iron, they were incubated with 0, 100, or 200 µg/mL ferric ammonium citrate (FAC) (MP Biomedicals) for 24 h.

Statistical analysis

Values are presented as mean ± standard error (n=6) unless otherwise indicated. Data were analyzed by one-way ANOVA and Tukey's multiple comparison post-hoc test (GraphPad Prism). Data sets with unequal variances were ln-transformed to normalize variance prior to statistical analysis.

Results

Iron status of rats

After 3 weeks of consuming their assigned diets, rats fed the iron-overloaded diet had hepatic non-heme iron concentrations (µg/g wet weight) that were 60-fold higher ($P < 0.001$) than those in iron-adequate controls (1812 ± 345 versus 30.1 ± 5.0), whereas rats fed the iron-deficient diet became anemic with hepatic non-heme iron concentrations that were 60% lower ($P < 0.01$) than those in controls (30.1 ± 5.0 versus 12.9).¹⁰ Hepatic total iron (heme and non-heme), measured by inductively coupled plasma mass spectrometry (ICP-MS), also demonstrated significantly different iron concentrations (µg/g dry weight) between the three groups (iron deficient: 93.2 ± 6.7 ; iron adequate: 267.8 ± 63.8 ; iron overload: 4966 ± 275.5).¹⁰ Parallel analysis of a sample of Bovine Liver Standard Reference Material 1577b (National Institute of Standards and Technology, NIST) confirmed the accuracy of liver iron measurements by ICP-MS. In iron-loaded rats, non-heme iron concentrations (µg/g) were also elevated in pancreas (18.7 ± 2.5 versus 4.7 ± 0.6 , $P < 0.001$) and heart (27.7 ± 1.1 versus 18.6 ± 2.1 , $P < 0.01$). In iron-deficient rats, non-heme iron concentrations in heart (13.6 ± 1.3 µg/g) and pancreas (4.6 ± 0.2 µg/g) were not significantly different from those in iron-adequate controls. ICP-MS analysis of pancreas revealed that total iron concentrations (µg/g dry weight) differed significantly between all three groups (iron deficient: 38.2 ± 2.3 ; iron adequate: 63.7 ± 5.8 ; iron overload: 162.7 ± 24.3).

Validation of the immunoreactivity of anti-ZIP14 antibody

To assess the immunoreactivity of our affinity-purified anti-ZIP14 antibody against rat ZIP14, we performed western blot analysis of lysates from HEK 293T cells transfected with pCMV-Sport2 (control) or pCMV-Sport6 containing rat ZIP14 cDNA. In cells transfected with rat ZIP14 cDNA (HEK + rZIP14), the anti-ZIP14 antibody detects unique bands at ~130 kDa and ~55 kDa (Figure 1A). In isolated rat liver membrane, the antibody detects a band at ~130 kDa

that aligns with the band obtained from HEK cells transfected with rat ZIP14. Immunoreactivity of the anti-ZIP14 antibody was abolished by preincubating the antibody with a 50-fold molar excess of peptide immunogen, indicating that the antibody is specific for ZIP14 peptide (Figure 1A). The ability of the antibody to recognize rat ZIP14 was further assessed by using immunoprecipitation and western blotting. Immunoprecipitation of HEK cells transfected with rat ZIP14 cDNA (HEK + rZIP14) or rat liver membrane resulted in the enhanced detection of the band at ~130 kDa (Figure 1B). Collectively, these data indicate that the immunoreactive band at ~130 kDa most likely represents rat ZIP14. Detection of rat liver ZIP14 at ~130 kDa is consistent with results reported for mouse liver.¹¹ Also, as for mouse liver, treatment of rat liver lysates with PNGase F reduced the apparent molecular mass of ZIP14 from ~130 kDa to ~100 kDa, indicating that the rat protein contains *N*-linked oligosaccharides (Figure 1C). To confirm the detection of ZIP14 in liver, pancreas, and heart, we performed western blot analysis of tissues from wild-type (WT) mice, *Zip14* knockout (KO) mice, and rats. In liver from WT mice and rats, the predominant immunoreactive band is detected at ~130 kDa along with a smear of high-molecular-mass bands (Figure 1D) likely representing glycosylated oligomers, as reported previously.¹¹ The band at ~130 kDa is not detected in tissues of *Zip14* knockout mice thus confirming that this band is ZIP14. ZIP14 in pancreas and heart was also detected at ~130 kDa. A number of other immunoreactive bands are detected, but they are

detected in *Zip14* knockout mouse tissues (Figure 1D and *Online Supplementary Figure S1*), indicating that they are non-specific. Therefore, for ZIP14 western blots, the immunoreactive band at ~130 kDa is shown.

Effect of iron deficiency and overload on ZIP14 and DMT1 expression in liver

Western blot analysis revealed that hepatic ZIP14 levels were 100% higher in iron-loaded rats than in iron-adequate controls (Figure 2A). The integral membrane protein scavenger receptor class B type I (SR-B1) was measured to indicate protein loading among lanes. In contrast to ZIP14, hepatic DMT1 levels were 70% lower in iron-loaded rats and 200% higher in iron-deficient rats compared with iron-adequate animals (Figure 2A). The immunoreactivity of the anti-DMT1 antibody and the position of the DMT1 immunoreactive band were validated by using tissues from *Dmt1* knockout animals (*data not shown*). Transferrin receptor 1 (TfR1) levels, which vary inversely with iron status,¹³ were measured as a positive control for iron-dependent changes in protein expression. As expected, TfR1 levels were up-regulated in iron deficiency and down-regulated in iron overload (Figure 2A). In iron-deficient animals, the up-regulation of DMT1 protein levels was associated with higher DMT1 mRNA levels [both the IRE (+) and the non-IRE (-) forms, Figure 2B], suggesting transcriptional regulation. Hcpidin mRNA levels, which vary in proportion to hepatic iron concentrations,¹⁴ were measured as a positive control for iron-dependent changes in mRNA expression.

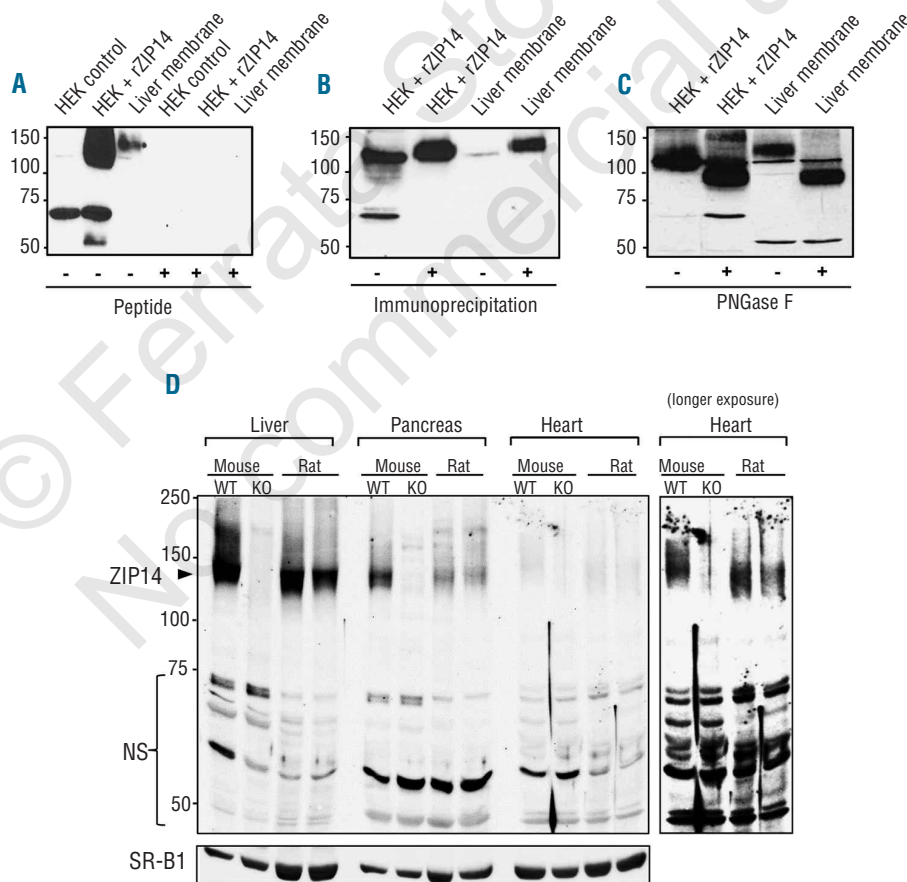


Figure 1. Characterization of the immunoreactivity of affinity-purified anti-ZIP14 antibody. (A) Western blot analysis of HEK 293T cells transiently transfected with empty pCMVSPORT2 vector (HEK control), HEK 293T cells transiently transfected with rat ZIP14 cDNA in pCMVSPORT6 (HEK + rZIP14), or rat liver membrane. Samples were analyzed after pre-adsorption of the anti-ZIP14 antibody with (+) or without (-) a 50-fold molar excess of ZIP14 peptide immunogen. (B) Western blot analysis of HEK 293T cells transiently transfected with rat ZIP14 cDNA in pCMVSPORT6 (HEK + rZIP14) or rat liver membrane with (+) or without (-) prior immunoprecipitation (IP) using the anti-ZIP14 antibody. (C) Western blot of non-IP samples in (B) after pre-incubating with (+) or without (-) PNGase F. (D) Western blot analysis of ZIP14 in liver, pancreas, and heart from wild-type (WT) mice, *Zip14* knockout (KO) mice, and rats. ZIP14-specific (arrowhead) and non-specific (NS) immunoreactive bands are indicated. To indicate lane loading, the blot was stripped and reprobed with the integral membrane protein SR-B1.

Effect of iron deficiency and overload on ZIP14 and DMT1 expression in pancreas

In pancreas, we found that ZIP14 levels were 70% higher in iron-loaded rats than in iron-adequate controls (Figure 3A). By contrast, DMT1 levels were unaffected by iron status. For the DMT1 western blot, pan-cadherin was used as a lane-loading control. Levels of TfR1 in the pancreas were higher in iron-deficient rats and lower in iron-loaded rats relative to iron-adequate controls. Levels of the non-IRE (-) form of DMT1 mRNA, but not the IRE (+) form, were lower in iron-loaded rat pancreas compared with iron-adequate pancreas (Figure 3B).

Effect of iron deficiency and overload on ZIP14 and DMT1 expression in heart

ZIP14 levels in heart were unaffected by iron status (Figure 4A). Only three iron-deficient and four iron-adequate heart samples were available for the final analysis of ZIP14 because most of the tissue was used up during western blot optimizations/modifications for heart, which expresses relatively low amounts of ZIP14 (Figure 1D). DMT1 levels were 4-fold higher in iron-deficient heart than in iron-adequate heart. As in liver and pancreas, cardiac TfR1 levels were higher in iron-deficient rats and lower in iron-loaded rats relative to iron-adequate controls. Although TfR1 levels were elevated in pancreas and heart, consistent with the well-known regulation of TfR1 by iron deficiency, non-heme iron concentrations were not found to be lower in these tissues. This apparent inconsistency is likely to be because TfR1 levels are regulated by the intracellular labile iron pool rather than the total pool of cellular non-heme iron.¹⁵ Changes in the labile iron pool, which represents only a small fraction of the total pool of cellular non-heme iron, may be manifest without detectable differences in the total pool of cellular non-heme iron, which is what we measured. Indeed, previous studies have shown that iron chelators can increase transferrin receptor levels without decreasing the concen-

tration of cellular non-heme iron.¹⁶ Despite marked up-regulation of DMT1 levels in iron-deficient heart, DMT1 mRNA levels were not elevated (Figure 4B), suggesting post-transcriptional regulation.

Immunofluorescence staining of ZIP14 in liver and pancreas

Immunofluorescence staining of rat liver sections revealed that ZIP14 is expressed throughout the liver lobule with no apparent zonal distribution (Figure 5A). ZIP14 staining was observed along the sinusoids (Figure 5B) at the basolateral membrane of hepatocytes (Figure 5C). In rat pancreas, ZIP14 was detected in acinar cells (Figure 5D), mostly as diffuse intracellular staining although some plasma membrane staining could be observed (Figure 5E). Diffuse intracellular ZIP14 staining was also detected in β -cells but the signal was markedly less intense than in acinar cells (Figure 5F). In agreement with the western blot findings regarding ZIP14 in rat liver and pancreas (Figures 2A and 3A), immunofluorescence staining of liver and pancreas sections consistently showed more intense ZIP14 staining in iron-loaded animals than in iron-adequate or iron-deficient animals (*Online Supplementary Figure S2*).

ZIP14 and DMT1 mRNA copy numbers in liver, pancreas, and heart

We previously reported that ZIP14 mRNA copy numbers were 10-fold greater than DMT1 copy numbers in HepG2 cells, a human hepatoma cell line.⁹ Here we compared the absolute copy number of ZIP14 and DMT1 transcripts in rat liver, heart, and pancreas. Among these tissues, ZIP14 is most abundantly expressed in liver whereas DMT1 is most abundantly expressed in pancreas. In liver, mRNA levels of ZIP14 were 3.4-fold greater than those of DMT1 (*Online Supplementary Figure S3*). In pancreas, mRNA levels of DMT1 were 3.8-fold greater than those of ZIP14. In heart, mRNA levels of ZIP14 and DMT1 were similar.

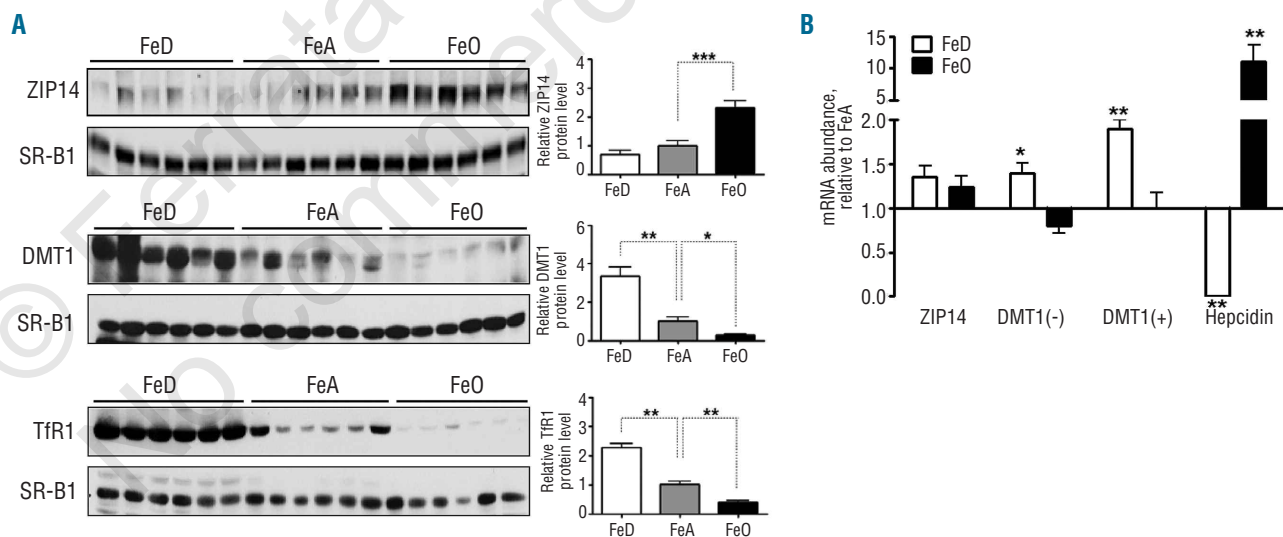


Figure 2. Effect of iron deficiency and overload on ZIP14 and DMT1 expression in liver. (A) Immunoblot analysis of ZIP14 and DMT1 in liver from iron-deficient (FeD), iron-adequate (FeA) and iron-overloaded (FeO) rats. Levels of TfR1, which vary inversely with iron status, were measured to demonstrate iron-dependent differences in protein expression. To indicate lane loading, blots were stripped and reprobed with SR-B1. Band intensities were quantified by densitometry and relative protein levels were normalized to the levels of SR-B1. (B) Relative mRNA levels of ZIP14 and DMT1 with (+) or without (-) IRE. Levels of hepcidin mRNA, which are positively regulated by iron, were measured to demonstrate iron-dependent differences in mRNA expression. Transcript abundances were normalized to the levels of cyclophilin mRNA. Values are means \pm SE, n=6. Asterisks indicate differences relative to FeA controls (* P <0.05, ** P <0.01).

Effect of genetic iron overload on ZIP14 and DMT1 levels in mouse liver and pancreas

To determine whether ZIP14 levels in liver and pancreas are up-regulated by iron overload in mouse as in rat, we examined tissues from hypotransferrinemic (hpx) mice, which develop genetic iron overload. Non-heme iron levels in liver were 135.1 ± 3.0 $\mu\text{g/g}$ (wt) versus 1658 ± 142 $\mu\text{g/g}$ (hpx) and those in the pancreas were 29.4 ± 3.0 $\mu\text{g/g}$ (wt) versus 191 ± 21 $\mu\text{g/g}$ (hpx). As in rat liver, ZIP14 levels in iron-loaded hpx mouse liver were 50% higher than those in WT controls (Online Supplementary Figure S4A). On the other hand, ZIP14 levels in hpx mouse pancreas were not up-regulated despite iron loading (Online Supplementary Figure S4B). DMT1 levels also did not differ between hpx and WT liver and pancreas (Online Supplementary Figure S4).

Effect of iron loading on ZIP14 levels in HepG2 hepatoma cells

Our data from iron-loaded rat and hpx mouse liver consistently showed that ZIP14 levels are elevated in iron overload. To determine whether ZIP14 levels are responsive to iron loading *per se*, we treated HepG2 cells, a human hepatoma cell line, with increasing concentrations of FAC, and then measured ZIP14 protein levels by western blot analysis. We found that ZIP14 protein levels in HepG2 cells increased in a dose-responsive fashion in response to FAC treatment (Figure 6). The iron-responsive ZIP14-immunoreactive band was detected at ~ 130 kDa, like that detected in rat and mouse liver. Levels of the iron-storage protein, ferritin (detected at ~ 20 kDa), were markedly elevated ($P < 0.001$) by FAC treatment, thus confirming cellular iron loading (Figure 6).

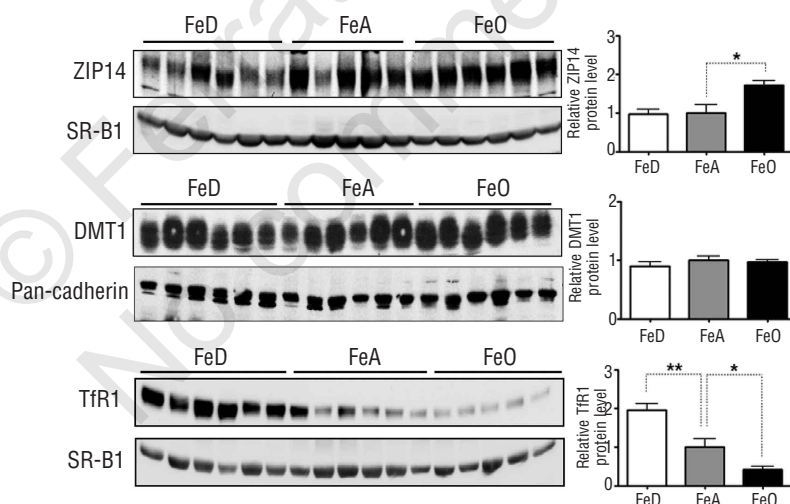
Discussion

In patients with iron overload, excess iron deposits pre-

dominantly in the liver, pancreas, and heart. As the primary site for body iron storage, the liver is usually the first organ affected, which is manifested clinically as fibrosis, cirrhosis, and hepatocellular carcinoma.¹⁷ Iron deposition in the pancreas is associated with β -cell destruction and diabetes mellitus.¹⁸ Iron loading of the heart, often a late complication of iron overload, is especially dangerous and remains the leading cause of death in patients with thalassemia major.¹⁹

Although NTBI is thought to be a main contributor to tissue iron loading, the molecular mechanisms that mediate NTBI uptake remain poorly defined.²⁰ DMT1 was first proposed to play a role in NTBI uptake by the liver by Trinder *et al.*,²¹ who reported that DMT1 was detectable at the plasma membrane of rat hepatocytes. Support for a role for DMT1 in NTBI uptake is provided by studies of human hepatoma cells transfected with DMT1²² and isolated hepatocytes from *Hfe* knockout mice.²³ However, DMT1 is a proton-coupled transporter that transports iron optimally at pH 5.5 and poorly at pH 7.5,^{24,25} suggesting that it would not function well at the hepatocyte cell surface facing blood plasma. More recently, Liuzzi *et al.*⁴ proposed that ZIP14 plays a role in liver NTBI uptake. This hypothesis was based on the following observations: (i) ZIP14 transports iron optimally at pH 7.5;⁴ (ii) ZIP14 is most abundantly expressed in the liver,³ (iii) ZIP14 localizes to the plasma membrane of hepatocytes,²⁶ and (iv) suppression of ZIP14 expression by siRNA reduced NTBI uptake by hepatocytes.⁴ The composition of plasma NTBI in iron overload appears to be heterogeneous, including not only ferric citrate⁵ but also protein-associated high-molecular-weight complexes that can be taken up by endocytosis.²⁷ Any NTBI taken up by endocytosis would subsequently require a transmembrane protein to translocate the iron from the endosome into the cytosol. It is possible that DMT1 and/or ZIP14 could function in this capacity as both have been detected in endosomes.^{9,28}

A



B

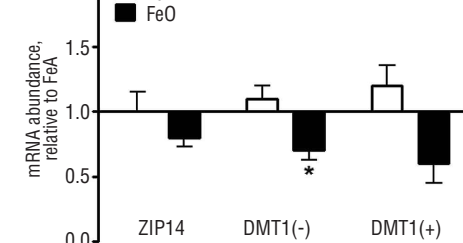


Figure 3. Effect of iron deficiency and overload on ZIP14 and DMT1 expression in pancreas. (A) Immunoblot analysis of ZIP14, DMT1, and TfR1 in pancreas from iron-deficient (FeD), iron-adequate (FeA) and iron-overloaded (FeO) rats. To indicate lane loading, blots were stripped and reprobed with SR-B1 or pan-cadherin. Band intensities were quantified by densitometry and relative protein levels were normalized to the levels of SR-B1 or pan-cadherin. (B) Relative mRNA levels of ZIP14 and DMT1 with (+) or without (-) IRE. Values are means \pm SE, $n=6$. Asterisks indicate differences relative to FeA controls (* $P < 0.05$, ** $P < 0.01$).

An important finding of the present study was that in iron-loaded rat liver ZIP14 levels were up-regulated whereas DMT1 levels were markedly down-regulated, suggesting that ZIP14 plays more of a role than DMT1 in iron overload. Such a possibility is strengthened by the fact that rat liver expresses at least 3-fold more ZIP14 mRNA than DMT1. That ZIP14 plays a role in iron overload is further supported by our observation that ZIP14 levels were up-regulated in livers of hpx mice, a genetic model of iron overload. Hpx mice are characterized by anemia and increased absorption of dietary iron, which deposits mainly in the liver. Hpx mice lack transferrin²⁹ and therefore any iron taken up by the liver is, by definition, NTBI.

The inverse regulation of DMT1 by iron suggests that DMT1 plays more of a role in iron-deficient than in iron-loaded liver. The up-regulation of both DMT1 and Tfr1 in iron-deficient liver is consistent with the proposed role of DMT1 in the transferrin cycle. The down-regulation of Tfr1 (and DMT1) in iron-loaded liver implies that transferrin iron uptake via Tfr1 decreases during iron overload.

The iron-dependent regulation of DMT1 we observed here contrasts with the findings in a study by Trinder *et al.*,²¹ who reported that DMT1 in rat liver is up-regulated by iron overload and down-regulated by iron deficiency. However a direct comparison of the two studies is complicated because we used western blot analysis to quantify relative DMT1 levels whereas Trinder *et al.*²¹ used immunohistochemistry.

Previous immunofluorescence studies using isolated primary mouse hepatocytes²⁶ and HepG2 hepatoma cells⁹ have detected ZIP14 at the plasma membrane and intracellularly. Here we performed immunofluorescence staining of rat liver sections and found that ZIP14 was broadly detected throughout the liver, with the expression being most abundant along the sinusoidal (basolateral) membrane of hepatocytes. The localization of ZIP14 to the sinusoidal membrane, which faces the blood, optimally positions ZIP14 to mediate the uptake of metal ions such as NTBI from the portal bloodstream.

ZIP14 may also play a role in NTBI uptake by the pancreas, as its levels were up-regulated in iron-loaded rats.

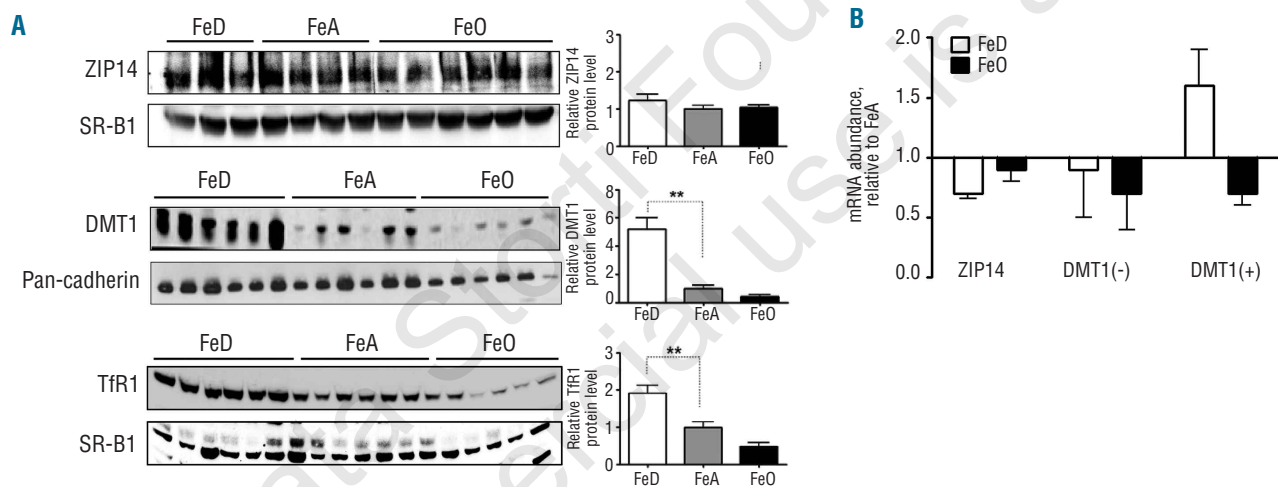


Figure 4. Effect of iron deficiency and overload on ZIP14 and DMT1 expression in heart. (A) Immunoblot analysis of ZIP14, DMT1, and Tfr1 heart from iron-deficient (FeD), iron-adequate (FeA) and iron-overloaded (FeO) rats. To indicate lane loading, blots were stripped and reprobed with SR-B1 or pan-cadherin. Band intensities were quantified by densitometry and relative protein levels were normalized to the levels of SR-B1 or pan-cadherin. (B) Relative mRNA levels of ZIP14 and DMT1 with (+) or without (-) IRE. Values are means ± SE, n=6. Asterisks indicate differences relative to FeA controls (**P*<0.05, ***P*<0.01).

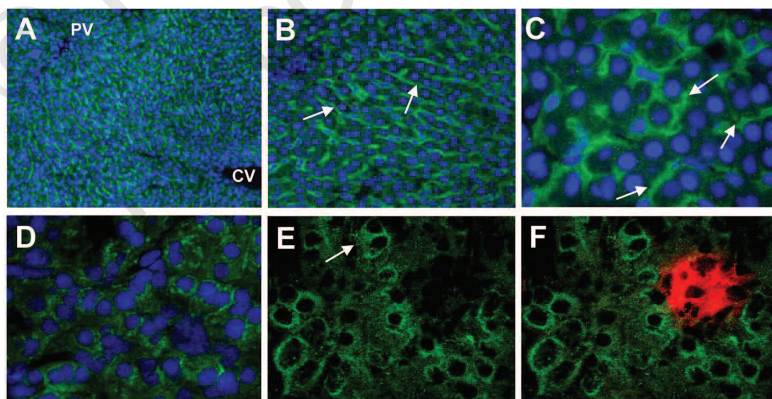


Figure 5. Immunofluorescence staining of ZIP14 in sections of rat liver and pancreas. (A) ZIP14 immunofluorescence (Alexa Fluor 488, green) and DAPI-stained nuclei (blue) in liver, original magnification ×10. The portal vein (PV) and central vein (CV) are indicated. (B) ZIP14 immunofluorescence, original magnification ×20. Arrows indicate staining along hepatic sinusoids. (C) ZIP14 immunofluorescence, original magnification ×60. Arrows indicate staining at the basolateral (sinusoidal) membrane of hepatocytes. (D) ZIP14 immunofluorescence (green) and DAPI-stained nuclei in pancreas, original magnification ×40. (E) ZIP14 immunofluorescence, original magnification ×60. The arrow indicates plasma membrane staining of an acinar cell. (F) ZIP14 immunofluorescence (green) with insulin staining (Alexa Fluor 594, red) in β-cells, original magnification ×60. Images were obtained by using a spinning disk confocal fluorescent microscope system.

Moreover, by using immunofluorescence staining, we detected ZIP14 mostly in acinar cells, the pancreatic cell type that preferentially loads iron during iron overload.^{8,30}

Interestingly, ZIP14 in acinar cells was detected diffusely throughout the cytosol and in vesicle-like structures, possibly representing early endosomes, where intracellular ZIP14 has been localized in HepG2 cells.⁹ Since early endosomes are formed from invagination of the plasma membrane, the orientation of ZIP14 would be preserved, and thus ZIP14 would be predicted to move iron into the cytosol. The iron could be either from endocytosed transferrin⁹ or from NTBI.²⁷ Although ZIP14 levels were up-regulated in the pancreas of iron-loaded rats, they were not up-regulated in the pancreas of iron-loaded hpx mice. The reason for this interspecies difference is not clear. One important difference between iron-loaded hpx mice and iron-loaded rats is that hpx mice are anemic,²⁹ which could introduce a confounding variable. Given that anemia, tissue iron overload, and plasma NTBI are also commonly found in transfusional and non-transfusional thalassemias, it will be important to determine the response of pancreatic ZIP14 in the context of thalassemia. The cellular distribution of ZIP14 in the pancreas is notably different from that of DMT1, which has been reported to localize primarily to pancreatic islet cells.³³ The localization of DMT1 to islet cells, along with its abundant expression in pancreas (i.e., 4-fold greater levels of DMT1 than ZIP14 transcripts), suggests that DMT1 may play an important role in iron uptake into β -cells of the pancreatic islets, which can be destroyed during iron overload.

The elevated ZIP14 protein levels observed in iron-loaded liver and pancreas were not associated with higher levels of ZIP14 mRNA, suggesting post-transcriptional regulation of ZIP14. Post-transcriptional regulation of iron-related proteins is often mediated through iron regulatory proteins that bind to iron-responsive elements located in mRNA, such as in ferritin and Tfr1.³⁴ ZIP14 mRNA, however, does not have an identifiable iron-responsive element in its mRNA and, therefore, is not likely to be regulated post-transcriptionally by iron regulatory proteins. Post-transcriptional regulation has been reported for a number of ZIP proteins including ZIP1,³⁵ ZIP3,³⁵ ZIP4,³⁶ ZIP5,³⁶ ZIP6,³⁷ ZIP7,³⁸ and ZIP8.³⁹ Precisely how these ZIP proteins are controlled post-transcriptionally is not well understood, but may involve a variety of mechanisms including translational inhibition, translational repression by miRNA, signal-induced translational activation, and

mRNA localization.^{40,41} Further studies are required to delineate how iron loading increases ZIP14 protein levels without affecting mRNA abundance.

Unlike in the liver and pancreas, ZIP14 levels in the heart were not up-regulated by iron overload, suggesting that the heart may have different NTBI uptake mechanisms. Possibilities include L-type Ca^{2+} channels,⁴² T-type Ca^{2+} channels,⁴³ or perhaps ZIP8, an iron and zinc transporter³⁹ that was reported to be up-regulated in heart tissue of thalassemic mice.⁴³ The lack of an effect of iron overload on heart ZIP14 levels might be due to heart-specific regulation or to the comparatively minor degree of iron loading in this tissue. The continued expression of ZIP14 during iron overload suggests that it was at least present to participate in NTBI uptake. On average, DMT1 levels in heart were lower in iron-loaded than in iron-adequate heart, but the difference did not reach statistical significance. Other studies have found that cardiac DMT1 levels were lower in iron-loaded animals than in controls.⁴⁴ Recently, Kumfu *et al.*⁴⁵ reported that NTBI uptake by cardiomyocytes was unaffected when the iron uptake activity of DMT1 or Tfr1 was blocked, indicating that DMT1 and Tfr1 are not required for NTBI uptake into these cells. In iron-deficient heart, DMT1 levels were up-regulated 4-fold whereas ZIP14 levels were not affected. The marked up-regulation of DMT1 implies that DMT1 plays an active role in iron acquisition by the heart, perhaps in concert with Tfr1, which was similarly up-regulated. Similar to a previous study,⁴⁴ the higher DMT1 protein levels in iron-deficient heart appear to result from post-transcriptional events because DMT1 mRNA levels were not higher.

The differential regulation of ZIP14, DMT1, and Tfr1 we observed in this study has several implications for tissue iron uptake in iron-related disorders such as iron deficiency and iron overload. First, during iron deficiency Tfr1 levels were up-regulated in liver, pancreas, and heart, indicating that these tissues are trying to enhance their uptake of iron from transferrin. This result was expected as it is likely a general phenomenon of all iron-deficient tissues. During iron deficiency DMT1 was also up-regulated in liver and heart, consistent with the model that DMT1 acts in concert with Tfr1 in the assimilation of iron from transferrin. In contrast, ZIP14 levels were not affected by iron deficiency in any tissue examined. This could mean that ZIP14 does not play a role in iron assimilation from transferrin or that ZIP14 does play a role,⁹ but that its levels are sufficient requiring no up-regulation.

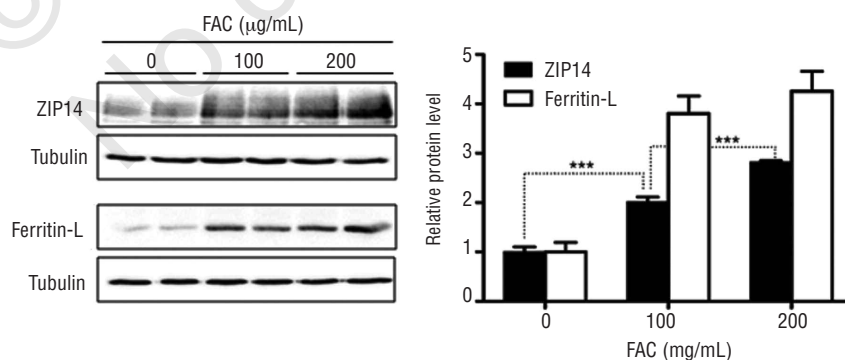


Figure 6. Cellular iron loading increases ZIP14 levels in HepG2 hepatoma cells. HepG2 cells were treated with the indicated concentrations of ferric ammonium citrate (FAC) for 24 h and lysates were analyzed for levels of ZIP14 and ferritin-L by immunoblot analysis. For SDS-PAGE, proteins were separated on a 7.5% or 12% polyacrylamide gel for ZIP14 and ferritin, respectively. To indicate lane loading, blots were stripped and reprobed with tubulin. Band intensities were quantified by densitometry and relative protein levels were normalized to the levels of tubulin. Values are means \pm SE of four independent experiments. Asterisks indicate difference relative to control (***) $P < 0.001$.

Second, during iron overload TfR1 levels were down-regulated in liver, pancreas, and heart, indicating diminished uptake of transferrin via TfR1. However, studies in mice have demonstrated that iron-loaded livers take up more iron from transferrin than do control livers.^{45,46} The greater uptake of transferrin iron is not mediated by TfR2, a TfR1 homologue abundantly expressed in liver, because iron-loaded TfR2 knockout mice also show enhanced uptake of iron from transferrin.⁴⁵ Thus, the iron-loaded liver possesses an alternative route of iron uptake from transferrin that is independent of transferrin receptors. Our results suggest that DMT1 does not participate in this alternate uptake pathway because it was markedly down-regulated in iron-loaded liver. ZIP14, on the other hand, was up-regulated in iron overload, suggesting that it may play a role in the assimilation of iron from transferrin. Indeed, studies in cultured cells provide evidence that ZIP14,⁹ and not TfR1 or DMT1,^{9,22,47} is limiting for iron assimilation from transferrin. Third, the up-regulation of ZIP14 and down-regulation of DMT1 in iron-loaded liver suggests that ZIP14 participates in NTBI uptake by the liver. Such a conclusion is independently supported by the recent functional characterization of ZIP14 expressed in *Xenopus* oocytes, which showed that the iron transport properties of ZIP14 are very similar to those reported for NTBI uptake by perfused rat liver and isolated hepatocytes.²⁵ In iron-loaded pancreas, it is possible that the up-regulation of ZIP14 may facilitate the uptake of NTBI into acinar cells, whereas DMT1 expressed in pancreatic islets would seem to be the primary candidate for NTBI uptake into β -cells.

The observation that ZIP14 levels were elevated in iron-loaded rat liver and pancreas could mean that ZIP14, by virtue of its ability to transport NTBI into cells, is a primary cause of iron loading in these tissues or that ZIP14 is simply responding to iron loading. Our data in HepG2 cells support the latter possibility in that iron loading was found to increase ZIP14 levels. Thus, it appears that iron loading *per se* increases ZIP14 levels, which could, in turn, increase the uptake of NTBI. Previous studies of HepG2 cells⁴⁸ and isolated rat and mouse hepatocytes^{23,49,50} have shown that iron loading increases the uptake of NTBI, and that this process is mediated by a protein carrier. Our data in HepG2 cells suggest that ZIP14 may represent this iron-responsive NTBI transporter. However, it should be pointed out that the response of ZIP14 to NTBI exposure in HepG2 cells or liver may not be applicable to ZIP14 in the pancreas and heart in some situations - for example in

chronically transfused patients with sickle cell disease. Such patients accumulate iron in the liver to levels observed in patients with thalassemia major but display less iron accumulation in the pancreas and heart, suggesting that NTBI uptake mechanisms may differ between the liver and extra-hepatic tissues.⁵¹

We recently reported that liver iron levels did not differ between *Zip14* knockout mice and controls.¹¹ These data, however, were pooled from mice of various ages (4, 8 and 16 weeks). Given that hepatic iron concentrations vary with age,⁵² the pooling of mice at different ages could obscure significant differences between groups. Indeed, recent comparisons of mice of the same age (4 weeks) revealed that hepatic iron concentrations were 40% lower ($P < 0.001$) in *Zip14* knockout mice ($n=8$) than in controls ($n=6$) (unpublished observations, S. Jenkitkasemwong and M. Knutson). Current studies are characterizing the iron status of *Zip14* knockout mice in detail at various ages.

In conclusion, these studies advance our understanding of how iron status regulates the expression of ZIP14 and DMT1 in the liver, pancreas, and heart. Knowledge of how these proteins are affected by iron deficiency and overload also provides some insight into their potential contributions to the assimilation of iron from transferrin and the uptake of NTBI. Current studies of mice lacking DMT1 and ZIP14 in specific cell types are evaluating the roles of these proteins to tissue iron uptake *in vivo*. Ultimately, a more complete understanding of how iron is taken up into cells will help to identify therapeutic targets for the treatment of iron-related pathologies.

Acknowledgments

We thank Dr. Toshio Hirano (Osaka University, Japan) for the generous contribution of the *Zip14* knockout mice and wild-type mice

Funding

This work was supported by research funding via grant R01 DK-080706 from the National Institute of Diabetes and Digestive and Kidney Diseases (NIDDK) to MDK, and from KAKENHI (#23592239) and the Kanagawa Nambyo Study Foundation to TF.

Authorship and Disclosures

Information on authorship, contributions, and financial & other disclosures was provided by the authors and is available with the online version of this article at www.haematologica.org.

References

- Gunshin H, Fujiwara Y, Custodio AO, Drenth C, Robine S, Andrews NC. Slc11a2 is required for intestinal iron absorption and erythropoiesis but dispensable in placenta and liver. *J Clin Invest*. 2005;115(5):1258-66.
- Fukada T, Kambe T. Molecular and genetic features of zinc transporters in physiology and pathogenesis. *Metallomics*. 2011;3(7):662-74.
- Taylor KM, Morgan HE, Johnson A, Nicholson RI. Structure-function analysis of a novel member of the LIV-1 subfamily of zinc transporters, ZIP14. *FEBS Lett*. 2005;579(2):427-32.
- Liuzzi JP, Aydemir F, Nam H, Knutson MD, Cousins RJ. Zip14 (Slc39a14) mediates non-transferrin-bound iron uptake into cells. *Proc Natl Acad Sci USA*. 2006;103(37):13612-7.
- Grootveld M, Bell JD, Halliwell B, Aruoma OI, Bomford A, Sadler PJ. Non-transferrin-bound iron in plasma or serum from patients with idiopathic hemochromatosis. Characterization by high performance liquid chromatography and nuclear magnetic resonance spectroscopy. *J Biol Chem*. 1989;264(8):4417-22.
- Breuer W, Hershko C, Cabantchik ZI. The importance of non-transferrin bound iron in disorders of iron metabolism. *Transfus Sci*. 2000;23(3):185-92.
- Craven CM, Alexander J, Eldridge M, Kushner JP, Bernstein S, Kaplan J. Tissue distribution and clearance kinetics of non-transferrin-bound iron in the hypotransferrinemic mouse: a rodent model for hemochromatosis. *Proc Natl Acad Sci USA*. 1987;84(10):3457-61.
- Iancu TC, Shiloh H, Raja KB, Simpson RJ, Peters TJ, Perl DP, et al. The hypotransferrinemic mouse: ultrastructural and laser microprobe analysis observations. *J Pathol*. 1995;177(1):83-94.
- Zhao N, Gao J, Enns CA, Knutson MD. ZRT/IRT-like protein 14 (ZIP14) promotes the cellular assimilation of iron from transferrin. *J Biol Chem*. 2010;285(42):32141-50.
- Nam H, Knutson MD. Effect of dietary iron

- deficiency and overload on the expression of ZIP metal-ion transporters in rat liver. *Biomaterials*. 2012;25(1):115-24.
11. Hojyo S, Fukada T, Shimoda S, Ohashi W, Bin BH, Koseki H, Hirano T. The zinc transporter SLC39A14/ZIP14 controls G-protein coupled receptor-mediated signaling required for systemic growth. *PLoS One*. 2011;6(3):e18059.
 12. Torrance JD, Bothwell TH. A simple technique for measuring storage iron concentrations in formalinised liver samples. *S Afr J Med Sci*. 1968;33(1):9-11.
 13. Lu JP, Hayashi K, Awai M. Transferrin receptor expression in normal, iron-deficient and iron-overloaded rats. *Acta Pathol Jpn*. 1989;39(12):759-64.
 14. Kautz L, Meynard D, Monnier A, Darnaud V, Bouvet R, Wang RH, et al. Iron regulates phosphorylation of Smad1/5/8 and gene expression of Bmp6, Smad7, Id1, and Atoh8 in the mouse liver. *Blood*. 2008;112(4):1503-9.
 15. Ponka P, Lok CN. The transferrin receptor: role in health and disease. *Int J Biochem Cell Biol*. 1999;31(10):1111-37.
 16. Trinder D, Batey RG, Morgan EH, Baker E. Effect of cellular iron concentration on iron uptake by hepatocytes. *Am J Physiol*. 1990;259(4 Pt 1):G611-7.
 17. Batts KP. Iron overload syndromes and the liver. *Mod Pathol*. 2007;20 (Suppl 1):S31-9.
 18. Utschneider KM, Kowdley KV. Hereditary hemochromatosis and diabetes mellitus: implications for clinical practice. *Nat Rev Endocrinol*. 2010;6(1):26-33.
 19. Borgna-Pignatti C, Rugolotto S, De Stefano P, Zhao H, Cappellini MD, Del Vecchio GC, et al. Survival and complications in patients with thalassemia major treated with transfusion and deferoxamine. *Haematologica*. 2004;89(10):1187-93.
 20. Brissot P, Ropert M, Le Lan C, Loreal O. Non-transferrin bound iron: A key role in iron overload and iron toxicity. *Biochim Biophys Acta*. 2012;1820(3):403-10.
 21. Trinder D, Oates PS, Thomas C, Sadleir J, Morgan EH. Localisation of divalent metal transporter 1 (DMT1) to the microvillus membrane of rat duodenal enterocytes in iron deficiency, but to hepatocytes in iron overload. *Gut*. 2000;46(2):270-6.
 22. Shindo M, Torimoto Y, Saito H, Motomura W, Ikuta K, Sato K, et al. Functional role of DMT1 in transferrin-independent iron uptake by human hepatocyte and hepatocellular carcinoma cell, HLF. *Hepatol Res*. 2006;35(3):152-62.
 23. Chua AC, Olynyk JK, Leedman PJ, Trinder D. Nontransferrin-bound iron uptake by hepatocytes is increased in the Hfe knockout mouse model of hereditary hemochromatosis. *Blood*. 2004;104(5):1519-25.
 24. Gunshin H, Mackenzie B, Berger UV, Gunshin Y, Romero MF, Boron WF, et al. Cloning and characterization of a mammalian proton-coupled metal-ion transporter. *Nature*. 1997;388(6641):482-8.
 25. Pinilla-Tenas JJ, Sparkman BK, Shawki A, Illing AC, Mitchell CJ, Zhao N, et al. Zip14 is a complex broad-scope metal-ion transporter whose functional properties support roles in the cellular uptake of zinc and nontransferrin-bound iron. *Am J Physiol Cell Physiol*. 2011;301(4):C862-71.
 26. Liuzzi JP, Lichten LA, Rivera S, Blanchard RK, Aydemir TB, Knutson MD, et al. Interleukin-6 regulates the zinc transporter Zip14 in liver and contributes to the hypozincemia of the acute-phase response. *Proc Natl Acad Sci USA*. 2005;102(19):6843-8.
 27. Sohn YS, Ghoti H, Breuer W, Rachmilewitz E, Attar S, Weiss G, Cabantchik ZI. The role of endocytic pathways in cellular uptake of plasma non-transferrin iron. *Haematologica*. 2012;97(5):670-8.
 28. Gruenheid S, Canonne-Hergaux F, Gauthier S, Hackam DJ, Grinstead S, Gros P. The iron transport protein NRAMP2 is an integral membrane glycoprotein that colocalizes with transferrin in recycling endosomes. *J Exp Med*. 1999;189(5):831-41.
 29. Trenor CC, 3rd, Campagna DR, Sellers VM, Andrews NC, Fleming MD. The molecular defect in hypotransferrinemic mice. *Blood*. 2000;96(3):1113-8.
 30. Horne WI, Tandler B, Dubick MA, Niemela O, Brittenham GM, Tsukamoto H. Iron overload in the rat pancreas following portacaval shunting and dietary iron supplementation. *Exp Mol Pathol*. 1997;64(2):90-102.
 31. Meynard D, Kautz L, Darnaud V, Canonne-Hergaux F, Coppin H, Roth MP. Lack of the bone morphogenetic protein BMP6 induces massive iron overload. *Nat Genet*. 2009;41(4):478-81.
 32. Rahier J, Loozen S, Goebbels RM, Abraham M. The haemochromatotic human pancreas: a quantitative immunohistochemical and ultrastructural study. *Diabetologia*. 1987;30(1):5-12.
 33. Koch RO, Zoller H, Theuri I, Obrist P, Egg G, Strohmayer W, et al. Distribution of DMT 1 within the human glandular system. *Histol Histopathol*. 2003; 18(4):1095-101.
 34. Muckenthaler MU, Galy B, Hentze MW. Systemic iron homeostasis and the iron-responsive element/iron-regulatory protein (IRE/IRP) regulatory network. *Annu Rev Nutr*. 2008;28:197-213.
 35. Wang F, Dufner-Beattie J, Kim BE, Petris MJ, Andrews G, Eide DJ. Zinc-stimulated endocytosis controls activity of the mouse ZIP1 and ZIP3 zinc uptake transporters. *J Biol Chem*. 2004;279(23):24631-9.
 36. Weaver BF, Dufner-Beattie J, Kambe T, Andrews GK. Novel zinc-responsive post-transcriptional mechanisms reciprocally regulate expression of the mouse SLC39A4 and SLC39A5 zinc transporters (Zip4 and Zip5). *Biol Chem*. 2007;388(12):1301-12.
 37. Taylor KM, Morgan HE, Smart K, Zahari NM, Pumford S, Ellis IO, et al. The emerging role of the LIV-1 subfamily of zinc transporters in breast cancer. *Mol Med*. 2007;13(7-8):396-406.
 38. Huang L, Kirschke CF, Zhang Y, Yu YY. The ZIP7 gene (Slc39a7) encodes a zinc transporter involved in zinc homeostasis of the Golgi apparatus. *J Biol Chem*. 2005;280(15):15456-63.
 39. Wang CY, Jenkitkasemwong S, Duarte S, Sparkman BK, Shawki A, Mackenzie B, Knutson MD. ZIP8 is an iron and zinc transporter whose cell-surface expression is up-regulated by cellular iron loading. *J Biol Chem*. 2012;287(41):34032-43.
 40. Besse F, Ephrussi A. Translational control of localized mRNAs: restricting protein synthesis in space and time. *Nat Rev Mol Cell Biol*. 2008;9(12):971-80.
 41. Gebauer F, Hentze MW. Molecular mechanisms of translational control. *Nat Rev Mol Cell Biol*. 2004;5(10):827-35.
 42. Oudit GY, Trivieri MG, Khaper N, Liu PP, Backx PH. Role of L-type Ca²⁺ channels in iron transport and iron-overload cardiomyopathy. *J Mol Med (Berl)*. 2006;84(5):349-64.
 43. Kumfu S, Chattapakorn S, Srichairatanakool S, Settakorn J, Fucharoen S, Chattapakorn N. T-type calcium channel as a portal of iron uptake into cardiomyocytes of beta-thalassemic mice. *Eur J Haematol*. 2011;86(2):156-66.
 44. Ke Y, Chen YY, Chang YZ, Duan XL, Ho KP, Jiang DH, Wang K, Qian ZM. Post-transcriptional expression of DMT1 in the heart of rat. *J Cell Physiol*. 2003;196(1):124-30.
 45. Chua AC, Delima RD, Morgan EH, Herbison CE, Timitz-Parker JE, Graham RM, et al. Iron uptake from plasma transferrin by a transferrin receptor 2 mutant mouse model of haemochromatosis. *J Hepatol*. 2010;52(3):425-31.
 46. Wilms JW, Batey RG. Effect of iron stores on hepatic metabolism of transferrin-bound iron. *Am J Physiol*. 1983;244(2):G138-44.
 47. Wetli HA, Buckett PD, Wessling-Resnick M. Small-molecule screening identifies the selenazal drug ebselen as a potent inhibitor of DMT1-mediated iron uptake. *Chem Biol*. 2006;13(9):965-72.
 48. Parkes JG, Randell EW, Olivieri NF, Templeton DM. Modulation by iron loading and chelation of the uptake of non-transferrin-bound iron by human liver cells. *Biochim Biophys Acta*. 1995;1243(3):373-80.
 49. Richardson DR, Chua AC, Baker E. Activation of an iron uptake mechanism from transferrin in hepatocytes by small-molecular-weight iron complexes: implications for the pathogenesis of iron-overload disease. *J Lab Clin Med*. 1999;133(2):144-51.
 50. Scheiber-Mojdehkar B, Zimmermann I, Dresow B, Goldenberg H. Differential response of non-transferrin bound iron uptake in rat liver cells on long-term and short-term treatment with iron. *J Hepatol*. 1999;31(1):61-70.
 51. Noetzli LJ, Coates TD, Wood JC. Pancreatic iron loading in chronically transfused sickle cell disease is lower than in thalassaemia major. *Br J Haematol*. 2011;152(2):229-33.
 52. Hahn P, Song Y, Ying GS, He X, Beard J, Dunaief JL. Age-dependent and gender-specific changes in mouse tissue iron by strain. *Exp Gerontol*. 2009;44(9):594-600.